Explorative Building of 3D Vessel Tree Models [1)]

Georg Langs[123], *Petia Radeva*[3], *Francesc Carreras*[4]

[1] Institute for Computer Graphics and Vision, Graz University of Technology, Inffeldgasse 16 2.OG, A-8010 Graz, Austria

[2] Pattern Recognition and Image Processing Group 183/2, Vienna University of Technology, Favoritenstr. 9, A-1040 Vienna, Austria langs@prip.tuwien.ac.at

[3] Computer Vision Center, Universitat Autònoma de Barcelona, Edifici 0, Campus UAB, Bellaterra, Spain, petia@cvc.uab.es

[4] Hospital St. Pau, Barcelona, Avda. Sant Antoni Maria Claret, 167 Barcelona 08025, Spain, fcarreras@hsp.santpau.es

Abstract:
This paper addresses the problem of segmenting vessels and other tubular tree-like structures. The underlying work was done in the context of interventional radiology where new CT technologies yield 3D data of high quality depicting the heart. It is highly desirable to make this information available during actual intervention. Before registering the 3D data to a sequence of live angiography images a parametrical model of the choronary vessel tree has to be calculated from the CT data.

The model is build by exploring the branching vessel tree starting from a single position and successively expanding through the vessels guided by a local deformable surface. The result is a tree of cylindrical segments each adapted to the vessel walls. It can then be registered to angiography images in a fast and robust way.

1 Introduction

Different approaches to segment 3D tubular data exist. In [2] vessel trees and medial axes are extracted by applying morphological methods yielding a voxel based identification of vessels. In [1] an approach to enhance the response of vesselness filters was presented. Deformable

[1)]This research has been supported by the Austrian Science Fund (FWF) under the grants P17083-N04, P14445-MAT and P14662-INF.

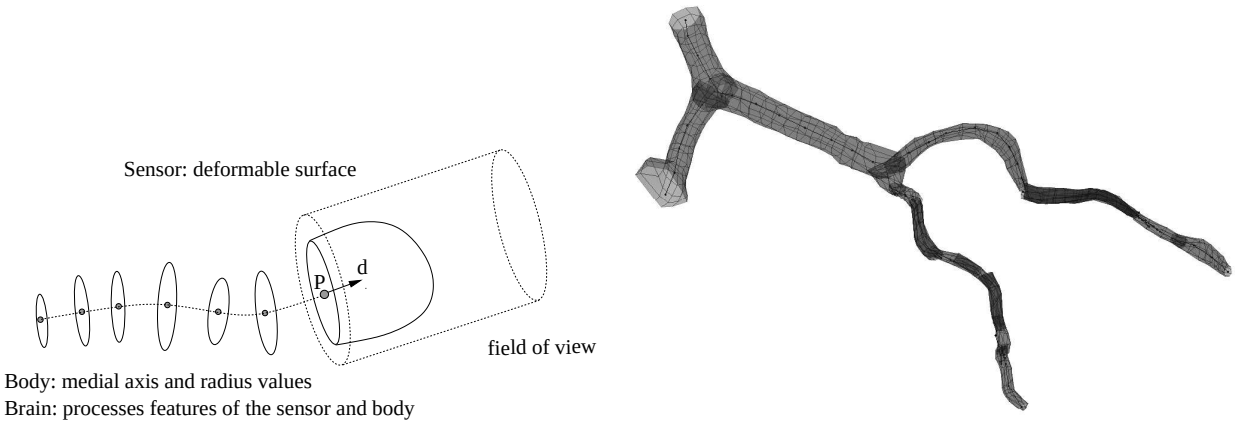

a. b.

Figure 1: a: Scheme of the local deformable model, the field of view, vessel medial axis and radius estimates. b: A resulting model of the coronary artery tree.

models are widely used in medical applications due to their robustness and the resulting explicit description of the entity of interest [8]. In [3, 6] a minimal cost path algorithm is used to perform an active contour search between two given points. In [7] deformable organisms are introduced. They are autonomous agents, that perform subsequent segmentation steps based on internal information and a sensory unit, that is aware of parts of or the entire data.

Instead of using a global model to guide the vessel segmentation, the organism uses knowledge of the local data and makes decisions affecting only its local behavior. This strategy is applied since the vessel trees form complex networks that make a reconstruction of the whole tree in a global way unfeasible. The decisions are based on the *sensed* local data and a behavioral model that enables the organism to draw conclusions from sensor input and its own body shape.

In this work we adopt a similar physics-based approach by exploring the vessel system with a local deformable model in order to successively build a parametric model of the vessel tree consisting of cylindrical segments. In Fig.1(b) an example of a resulting model is depicted. Vessel bifurcations are detected based on the form of the exploring balloon and knowledge about the body shape. In contrast to [7] the organism branches and grows within 3D data.

The paper is organized as follows: In section 2 the method to build a vessel tree model is described in detail, in section 3 results are discussed and section 4 gives a summary and suggestions for future directions of the work.

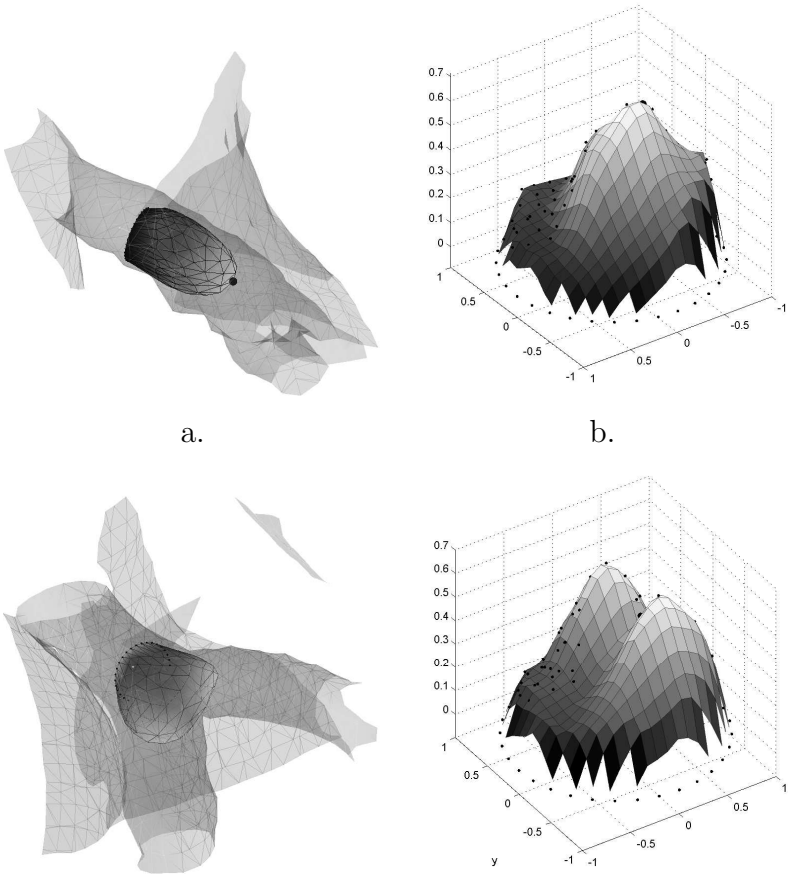

Figure 2: Explorer head and corresponding curvature values: a. and b.: within a vessel, c. and d.: detecting a vessel bifurcation

2 Methodology

Enhancing the vessels First the initial CT data $\mathbf{I}$ is filtered in order to enhance the contrast of tubular structures. We use a vesselness filter as introduced in [5]. It is based on the eigen value analysis of the Hessian matrix evaluated on positions within the volume. A vessel likeliness function can then be defined on different scales corresponding to different vessel radii. By combining the responses a new volume $\mathbf{I}^{\mathbf{v}}$ is generated.

An organism travelling through the vessel system Starting from a single manually indicated position and a corresponding direction the search through the vessel tree proceeds by inflating a deformable surface driven by a directed pressure force. Fig.1(a) depicts the scheme of the organism travelling through the vessels. The local deformable surface serves as *sensor* in the 3D data, the model that has been build already consitutes the *body* of the organism. Features from both are used as input for the algorithm or the *brain* that builds the model.

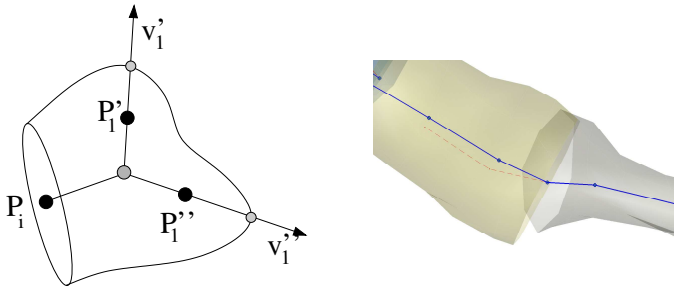

a. b.

Figure 3: a. Two new segments are initialized at a detected bifurcation; b. false segments (dashed lines) are pruned.

Due to the highly elongated shape of vessels a local strategy is reasonable, since after vessel walls have been detected, there is no significant improvement expected at these positions while the processing power can be concentrated on the front, namely the explorer balloon, which makes its progress through the vessel. Hence the model grows only on the surface of the explorer balloon instead of its entire surface. Thereby in a first step a sequence of medial axis points and corresponding diameters is generated.

Proceeding step by step The building procedure starts from a given position $\mathbf{P}_i$ in the direction $\mathbf{d}_i$. The deformable parameterized surface $\mathbf{x}(s,r) = (\mathbf{x}_1(s,r), \mathbf{x}_2(s,r), \mathbf{x}_3(s,r))$ is initialized as a triangular mesh filling a circle with radius r_i. During the deformation of the surface which constitutes the explorer balloon the energy functional

$$E(\mathbf{x}) = E_{int}(\mathbf{x}) + E_{ext}(\mathbf{x}) + E_{pr}(\mathbf{x}) \tag{1}$$

is minimized according to [4]. Only a part of the entire data, the *field of view*, is used for the deformation of the explorer balloon. This focuses the optimization on a region where substantial progress can be expected. After the optimization procedure for the deformable model has converged a new point $\mathbf{P}_{i+1}$ on the medial vessel axis and a corresponding diameter estimate $\mathbf{d}_{i+1}$ are calculated from the resulting surface.

Utilizing sensor input and memory The deformable model formulation used in this work follows the one introduced in [8], finite element based solutions in 2 and 3 dimensions are explained in detail in [4]. In the following only a short overview is given, for more details please refer to [4].

$$\mathbf{F_{pr}} = k_1\mathbf{n}(r,s) + k_2\mathbf{d}. \tag{2}$$

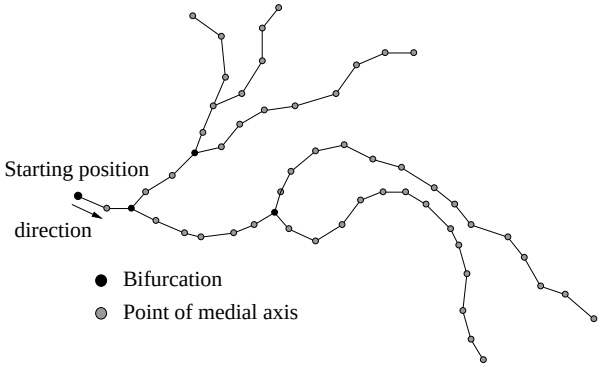

Figure 4: The tree structure

The internal energy $\mathbf{E_{int}}$ is established by internal elasticity and rigidity properties of the balloon surface. $\mathbf{E_{pr}}$ is determined by the directed pressure force $\mathbf{d}$ defined in Eq.2, where $\mathbf{n}$ is normal to the surface, and k_1 and k_2 are parameters to steer the surface behavior.

$\mathbf{E_{ext}}$ is derived from the CT data $\mathbf{I}$ weighted with $\mathbf{I^v}$. It is thresholded at a value corresponding to the expected Hounsfield number within the vessels after contrast fluid has been applied. On the resulting data a distance transform is performed resulting in $\mathbf{I}^d$ and a corresponding *distance potential force field* [4] $E_{ext} = -|\nabla \mathbf{I}^d|^2$.

The knowledge concerning detected medial axes and radius values during the vessel building allows for an immediate pruning of false multiple vessel segments that occur due to insufficient contrast fluid presence or sharp vessel turns. This would lead to false bifurcations but exploration of segments is stopped if for a new position $\mathbf{P}$: $\|\mathbf{P} - \mathbf{P}'_i\| < r'_i$ holds for any $\mathbf{P}'_i$ part of the existing vessel segments.

Fig.3(b) shows a false bifurcation within a vessel and the resulting medial axis. It is pruned because of the proximity to the already existing vessel segment.

Detecting bifurcations The internal energy $\mathbf{E_{int}}$ can also be used to determine local information on the curvature of the surface after it has been addapted to the CT data. Fig.2 shows explorer balloons (a) within a vessel and (c) confronting a bifurcation in the vessel structure, in Figs.2(b) and (d) local curvatures of the surfaces are plotted over the surface parameterization. Multiple local maxima can be used as indicator for branchings. At a detected bifurcation the old segment is finished and the corresponding cylinder in the model undergoes a final addaption process to the vessel walls. Starting from its end two vessel segments are initialized based on the form of the last explorer balloon within the bifurcation (Fig.3(a)).

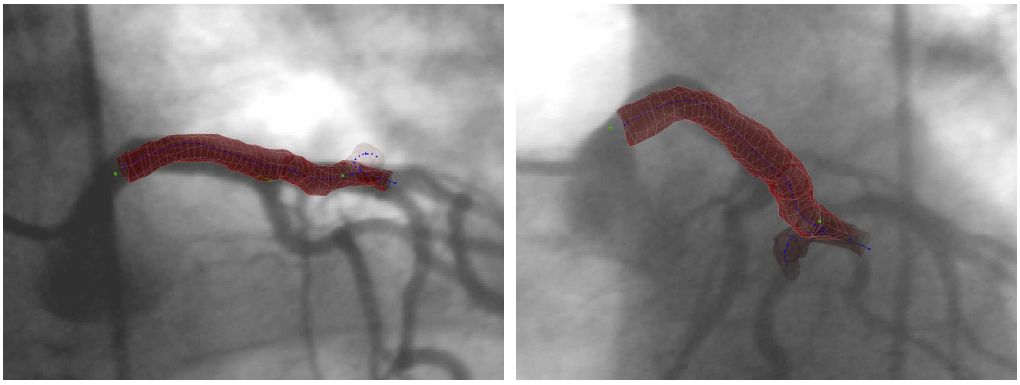

Figure 5: Vessel tree model registered to two different angiography projections taken during intervention

The vessel tree After multiple segments have been build, they are connected to a vessel tree, that makes direct navigation possible, since it contains explicit knowledge about connectivity, distances and shape of the investigated part of the vessel system. Fig.4 shows the scheme of a tree model. Vessel medial axes are depicted.

3 Results

To evaluate our approach we acquired a set of CT data of 8 patients using a Toshiba Aquilion 16 multislice sanner [9]. The data had a spatial resolution of 0.49 $\times$ 0.49 $\times$ 0.6mm. It was acquired during the diastolic phase of the heart beat and vessel trees were build for the left coronary artery. In order to judge the quality of the results for each patient models and filtered CT volumes of the left coronary artery were registered to two X-ray images taken from different viewing angles. Again images recorded during the diastolic phase were used. The pairs provided sufficient accuracy for navigation by means of the match between the vessels in the two modalities. In favor of an easier comprehension of the 3D spatial structure of the vessels ambiguities present in the angiography could be reduced by the superimposed model. Due to overlapping structures in the angiography in 2 cases the landmark identification was difficult and interactive correction was necessary. In Fig.5 a pair of two X-ray images of the same patient taken under different viewing angles is depicted together with the registered model of the coronary artery.

Model building is robust against noise but can suffer from calcium saturation in CT images causing vessel structures seeming to merge. Poor contrast in the CT data can cause a larger number of false bifurcations and premature endings of vessel segments. Although the false segments can be pruned this causes increased computation time.

During registration to angiography data registering models proved to be significantly faster than registering volume data due to the decreased number of points. Fig.6 shows a resulting

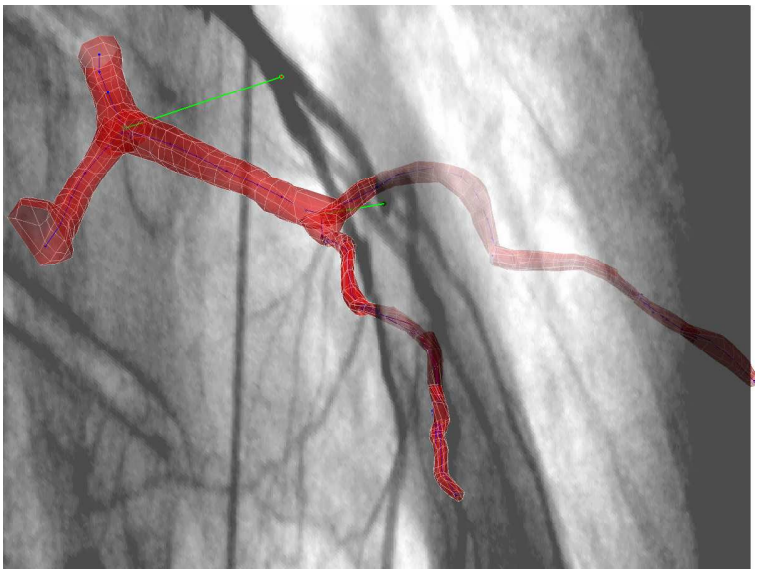

Figure 6: Registered vessel tree model

model of a left coronary artery registered to an angiography taken during intervention. Two point pairs used for computing the registration transformation are connected with lines.

4 Conclusion

A method to build 3D models of branching vessel trees from CT data is introduced. The model building process is local and starts from a single point and direction. The work is part of a project on multi modal vessel registration. Future research will focus on fastening the model building process and the projection of a tracked catheter position in the angiography onto the model during intervention. The quality of the tree model is expected to improve if more advanced techniques are used for the bifurcation detection based on the explorer balloon. The organism architecture allows for a straight forward integration. Resulting models of the vessel tree can be object to non rigid registrations as presented in [10].

References

[1] Reinhard Beichel, Thomas Pock, Christian Janko, Roman Zotter, Bernhard Reitinger, Alexander Bornik, Kalman Palagyi, Erich Sorantin, Georg Werkgartner, Horst Bischof, , and Milan Sonka. Liver segment approximation in ct data for surgical resection planning. In *Proceedings of SPIE 2004*, 2004.

[2] Z. Chen and S. Molloi. Automatic 3d vascular tree construction in ct angiography. *CMIG*, 27:469–479, 2003.

[3] L. Cohen and R. Kimmel. Global minimum for active contour models: A minimal path approach. In *Proc. CVPR*, pages 666–673, 1996.

[4] L. D. Cohen and I. Cohen. Finite element methods for active contour and ballons for 2d and 3d images. *Trans. PAMI*, 15:1131–1147, November 1993.

[5] A. F. Frangi, W.J. Niessen, K.L. Vincken, and M.A. Viergever. Multiscale vessel enhancement filtering. In *Proc. MICCAI*, number 1496 in LNCS, pages 130–137, 1998.

[6] A.F. Frangi, W.J. Niessen, R.M. Hoogeveen, Th van Walsum, and M.A. Viergever. Model-based quantitation of 3d magnetic resonance angiographic images. *IEEE TMI*, 18(10):946–956, 1999.

[7] G. Hamarneh, T. McInerney, and D. Terzopoulos. Deformable organisms for automatic medical image analysis. In *Proc. MICCAI*, 2001.

[8] M. Kass, A. Witkin, and D. Terzopoulos. Snakes: Active contour models. *IJCV*, 1:321–331, 1988.

[9] Ruben Leta, Francesc Carreras, Xavier Alomar, Joan Monell, Joan Garcia-Picart, Josep M. Auge, Anonio Salvador, and Guillem Pons-Llado. Non-invasive coronary angiography with 16 multidetector-row spiral computed tomography: a comparative study with invasive coronary angiography. *Rev. Esp. Cardiol*, 57(3):217–224, 2004.

[10] C. Twining and S. Marsland. Constructing diffeomorphic representations of non-rigid registrations of medical images. In *Proc. IPMI*, LNCS 2732, pages 413–425, 2003.